of the inner region occurs similarly for large or small δ. The contrast in flux (and thus the RMS amplitude of the modulation) is thus larger for larger δ, explaining the trend.

LINK WITH OBSERVATIONS

Because the modulation comes from shadowing, the disc inclination angle θ is important in determining the maximum shadowing and thus the maximum RMS amplitude that a given choice of parameters can produce. Motivated by a comparison with the LFQPOs of GRS 1915+105 (see *e.g.* the review [2]), we again focus on the parameter choices of simulation #8 and vary the inclination angle to obtain different values of the RMS amplitude. As expected, the more edge-on the view, the higher the RMS amplitude. Present observational data are insufficient to definitively confirm or contradict the predicted behavior. Such a trend could explain the absence of LFQPO in Cyg X-1, as the RMS amplitude expected from the inferred inclination angle is very small. More objects with a wider range of inclination angles are needed.

CONCLUSION

The key effect of the asymmetry from our blob or spiral structure that produces the LFQPO is the shadowing of the disk's inner region by the structure. The RMS amplitude of the modulation increases as the height contrast between the spiral or blob becomes sharper. We considered only symmetric height profiles of the structure, but it is the steepness of the slope in the inner edge of the structure that is most important–the sharper the rise, the stronger the shadowing for a fixed maximum height.

We also found that there is an optimal radius where a given non-axisymmetric structure is most effective at producing the LFQPO RMS amplitude: If the structure is too close to the central engine, then too little of the most luminous part of the disk would be shadowed. On the other hand, if the structure is too far from the center, then it is ineffective at shadowing the the most luminous part. This will have to be compared with observations.

REFERENCES

1. Chakrabarti, S. K., & Manickam, S. G. 2000, ApJ, 531, L41
2. McClintock J. E. & Remillard, R. A., "Compact Stellar X-ray Sources," eds. W.H.G. Lewin and M. van der Klis, Cambridge University Press.
3. Remillard, R. A., Muno, M. P., McClintock, J. E., Orosz, J. A. 2002, ApJ, 580, 1030
4. Stella, L. & Vietri, M. 1998, ApJ, 492, L59
5. Tagger, M., and Pellat, R., 1999, A&A, 349, 1003 (TP99)
6. Tomsick, J.A. and Kaaret, P., 2001, ApJ, 548, 401.
7. Varnière, P. and Tagger M., 2002, A&A, 394, 329-338.

20

Time and spectral changes of GRS 1915+105 in the ρ class

G. Ventura*, E. Massaro*, T. Mineo†, G. Cusumano†, M. Litterio**, M. Feroci**, P. Casella‡ and G. Matt§

*Department of Physics, Univ. La Sapienza, Roma, Italy
†INAF, IASF, Palermo, Italy
**INAF, IASF, Roma, Italy
‡Astronomical Observatory of Roma, M. Porzio Catone, Italy
§Department of Physics, Univ. Roma Tre, Roma, Italy

Abstract. We report the results of the temporal and spectral analysis of the longest *BeppoSAX* pointing (about 770 ks) of the microquasar GRS 1915+105, performed in October 2000. The source was mainly observed in the variability class ρ characterized by series of sharp pulses with a typical recurrence time of about 50 s. This behaviour was generally stable but, occasionally, it changed to a more irregular state. A spectral analysis of the 1-100 keV emission showed a small but significant change of the disk temperature between the regular and irregular ρ-mode

Keywords: X-ray sources, Microquasar: GRS 1915+105
PACS: 95.85.Nv, 97.10.Gz, 97.80.Jp

INTRODUCTION

The X-ray emission of GRS 1915+105 is characterized by very different time and spectral behaviors grouped by Belloni et al. (2000) in 12 classes. In particular, the ρ class consists of quasi–periodic 'flares' recurring on a time scale of 1–2 minutes. Their typical shape shows a nearly exponential rising branch followed by a short maximum and a quite fast decay. In this contribution we present some preliminary results of a long wide band X-ray observation of GRS 1915+105 performed with the BeppoSAX satellite from 20 to 29 October 2000. We can define two modes of the ρ class from the MECS (2–10 keV) and PDS (13–200 keV) light curves, characterized by a limited but significant change of the mean spectral parameters.

THE LIGHT CURVES

During the observation of October 2000 the source behavior was for a large fraction of the time in the ρ class alternating stables and irregulars phases. In the final part of the pointing a transition to the ν class was observed. We divided the entire observation in segments each one approximately corresponding to a satellite orbit. Each segment was studied using the Discrete Fourier Transform (DFT) and the wavelet power spectra (WPS), however here we present the results on only two segments of a duration of 2000 s, indicated as *A* and *B*. Their MECS light curves, integrated in a time bin of 0.5 *s*, are plotted in the Fig. 1a, b, respectively. In the segment *A* pulses repeat regularly with a

CP797, *Interacting Binaries: Accretion, Evolution, and Outcomes*,
edited by L. Burderi, L. A. Antonelli, F. D'Antona, T. Di Salvo,
G. Luca Israel, L. Piersanti, A. Tornambè, and O. Straniero

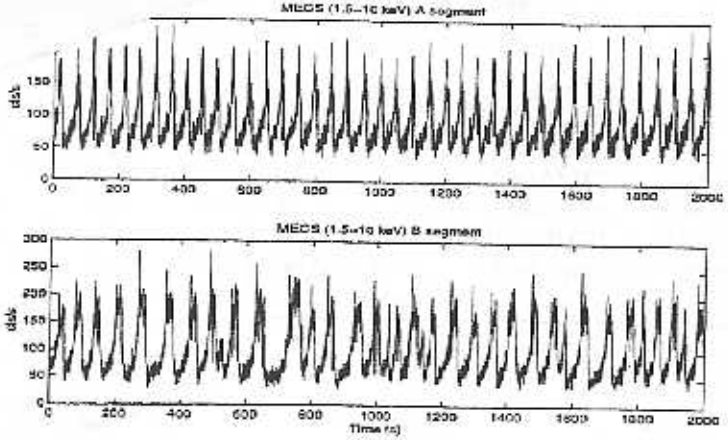

FIGURE 1. MECS light curves of the time segments A and B showing the *regular* and *irregular* modes of the ρ variability class.

stable pattern, while those of B have a variable recurrence time and show also different widths.

THE 2 MODES OF THE ρ CLASS

The DFT power spectra of the A time series in the MECS and PDS energy bands show a single prominent feature at the frequency of 20.28 mHz (corresponding to a recurrence time of 49.30 s). In the spectra of the B series there are two peaks at 14.11 mHz (70.87 s) and 16.56 mHz (60.37 s). WPS, computed by means of the Morlet wavelet transform, show that the A data set is characterized by an uninterrupted line of the maxima, centred at the period value of 49 s. Another line, but with a smaller power, is also present at ~24.5 s (the first harmonic). Both lines have a small amplitude oscillating behavior over a time scale of a few cycles because of the not precisely periodic recurrence of the pulses. WPS spectra of the B segments have a maximum line showing meanderings and interruptions in the interval 50–120 s. In the last part an isolated maximum appears at ~40 s. (see Fig. 2).

The use of DFT and WPS allows us to define a criterion, based on the number of peaks and the structure of the highest power line, to distinguish two *modes* of the ρ variability class: segments with spectra having a single prominent peak in the DFT power spectrum and a narrow and uniform strip in the WPS correspond to that we called *regular ρ mode*; segments with two or more high peaks in the DFT spectrum and WPS showing a winding path with bifurcations and/or isolated maxima are typical of the *irregular ρ mode*.

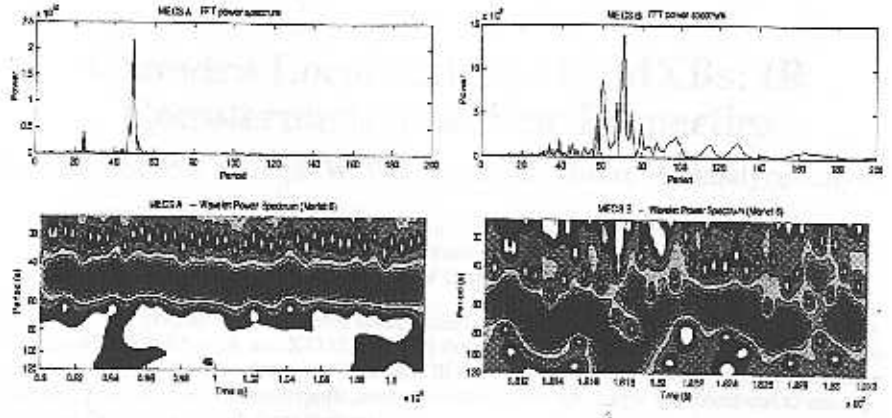

FIGURE 2. DFT and WPS power spectra for MECS A (left panels) and B (right panels) data series.

CHAOTIC BEHAVIOR ANALYSIS

For a more complete description of the two modes of the ρ class we investigated if the source behavior can be considered deterministic or chaotic calculating the *correlation integral* of Grassberger and Procaccia (1983):

$$C_M(R) = [N(N-1)]^{-1}\Sigma_i\Sigma_j H(R-|x_i-x_j|) \qquad (1)$$

where x_i and x_j are the data vector in a M dimensional phase space, computed at the instants t_i and t_j, respectively, H is the Heaviside function and R is a distance. The correlation dimension $D_2(M)$ can be estimated from the log-derivative of $C_M(R)$ with respect to R. We found that for the A data set $D_2(M)$ converges rapidly to a value close to 2. For the B series $D_2(M)$ doesn't converge to a finite value and increases above 5 (Fig. 3). We conclude then that while the *regular* ρ mode can be described by a small number of dynamical equation, the *irregular* ρ mode is somewhat of *intermediate* between a stochastic and a deterministic behavior.

SPECTRAL ANALYSIS

Spectral analysis was performed on the entire data sets to verify whether the mean emission changes in the two modes. We considered the events in MECS and PDS energy bands and used a two component model: *i*) a multitemperature blackbody accretion disk (*diskbb*) and *ii*) a logarithmic parabolic law $F(E) = K_n E^{-(\Gamma+\beta Log E)}$ for the high energy emission. Interstellar absorption from an equivalent hydrogen column density was fixed at $N_H = 5 \times 10^{22}$ cm^{-2} and the MECS/PDS intercalibration factor was limited in the range (0.82–0.88). Best fit values of the spectral parameters and their 1σ errors for the two data sets A and B are given in Table 1.

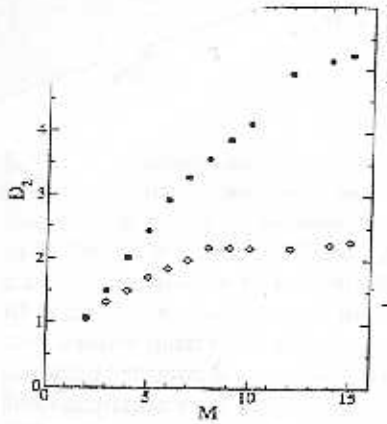

Table 1

	(ρ_{reg})	(ρ_{irr})
kT_{in}(keV)	1.601 (0.009)	1.764 (0.012)
K_d	182.4 (5.5)	116.6 (3.6)
K_b	3.60 (0.19)	3.74 (0.17)
Γ	1.64 (0.04)	1.59 (0.05)
β	0.41 (0.02)	0.47 (0.03)
$\chi^2_r/d.o.f.$	1.09 / 185	1.22 / 168
$F(2-10\,keV)^a$	1.74	1.77

a: 10^{-8} erg/(cm^{2}s)

FIGURE 3. Correlation dimensions for the A and B data sets. Table with the best fit spectral parameters

Note that the high energy component is unchanged while the B data have a disk temperature higher than A of ~10%. Although small this difference is significant because when the spectral model for A series is applied to B data the resulting χ^2 is 6.90.

CONCLUSIONS

Our analysis of the long BeppoSAX observation of October 2000 of GRS 1915+105 showed that the ρ variability class (Belloni et al. 2000) presents two modes. In the *regular* mode the distribution of the recurrence times of pulses has a small variance, power spectra have a single prominent peak and the WPSs show a narrow feature. In the *irregular* mode the distributions of recurrence times have a large variance, DFT spectra have two or more prominent peaks and the WPSs show features with meanderings, bifurcations and isolated maxima.

We also found that the mean emission spectrum of the ρ_{irr} mode has a higher inner disk temperature than ρ_{reg}. It is interesting that the source luminosity does not differ between the two data sets. In fact, the ratio between *diskbb* normalisation factors is nearly equal to inverse of the fourth power of the temperature ratio, also shown by the equal values of the 2– 10 keV fluxes. It is unclear what is the physical process triggering the mode change: the change of the dimension of the time series from about 2 to a higher values suggests that non-linear effects should be important in the system physics.

REFERENCES

1. Belloni T., Klein-Wolt M. et al. *Astron. Astrophys.*, **355**, 271 (2000).
2. Grassberger P., Procaccia I. *Physica*, **9D**, 189 (1983)

Chandra Localizations of LMXBs: IR Counterparts and their Properties

Stefanie Wachter*, Joseph W. Wellhouse† and Reba M. Bandyopadhyay**

*Spitzer Science Center, Caltech
†Harvey Mudd College
**Oxford University

Abstract. We present new Chandra observations of the low mass X-ray binaries (LMXBs) X1624−490, X1702−429, and X1715−321 and the search for their Infrared (IR) counterparts. We also report on early results from our dedicated IR survey of LMXBs. The goal of this program is to investigate whether IR counterparts can be identified through unique IR colors and to trace the origin of the IR emission in these systems.

Keywords: low mass X-ray binaries, infrared counterparts
PACS: 97.80.Jp

INFRARED PROPERTIES OF LMXBs

Traditionally, LMXBs have been studied in the optical and UV part of the spectrum. In order to explore the IR properties of LMXBs and to investigate the most heavily absorbed sources in the Galactic Bulge, we are undertaking a dedicated IR survey of all LMXBs. In addition to our own observations, we have also searched the literature for published IR magnitudes for these sources. For the brightest LMXBs in fields with moderate crowding, we extracted J, H, and K magnitudes from the 2MASS database. Selected early results from our survey are summarized in Table 1 below. Most of the observations were obtained with the 1.5m telescope at CTIO. Photometry was performed with DAOPHOT II and standardized magnitudes were derived through comparison with 2MASS.

Figure 1 shows the position of the individual LMXBs in the IR color-color diagram (filled circles). Open circles indicate multiple measurements of the same sources. Also shown are the main sequence and giant branch tracks. The intrinsic variability of the LMXBs limits the predictive power of the IR colors (see e.g. Sco X−1). A few sources reveal the contribution of a giant mass donor. X1608−52 and X1636−536 appear to show very unusual colors. These are some of the faintest sources we measured and require deeper observations to confirm our photometry.

Figure 2 shows the positions of the individual LMXBs in the IR color-magnitude diagram (note that apparent, not absolute, K magnitudes are plotted). The symbols are the same as used in Figure 1. For comparison, we also include the location of field stars from a representative Galactic Bulge field (small filled circles). The different branches visible in the color-magnitude diagram distinguish different types of stars. The first branch, roughly up to $J-K=1.8$, corresponds to nearby main sequence stars, while the clump of stars around $J-K=2.0-2.5$ represents a superposition of giant stars

CP797, *Interacting Binaries: Accretion, Evolution, and Outcomes*,
edited by L. Burderi, L. A. Antonelli, F. D'Antona, T. Di Salvo,
G. Luca Israel, L. Piersanti, A. Tornambé, and O. Straniero